Electronic Supplementary Material (ESI) for Physical Chemistry Chemical Physics.

Supporting information for: Cation influence on heterocyclic ammonium ionic liquids: a molecular dynamics study

Promit Ray[1], Roman Elfgen[1,2], and Barbara Kirchner[1*]

[1] *Mulliken Center for Theoretical Chemistry, Rheinische Friedrich-Wilhelms-Universität Bonn, Beringstr. 4+6, D-53115 Bonn, Germany*

[2] *Max Planck Institute for Chemical Energy Conversion, Stiftstr. 34–36, D-45470 Muelheim an der Ruhr, Germany*

E-mail: kirchner@thch.uni-bonn.de

*To whom correspondence should be addressed

1 Computational Details

Table S1: Comparison of experimental and isobaric-isothermal densities (g/cc) with scaled charges. NPT-densities with unscaled charges are also presented for the pure ILs and the 0.1 M doped solutions for comparison.

System	Expt.	NPT (+/- 0.8)	Error %	NPT (+/- 1)
$[pipHH]^+$	1.541	1.569	1.817	1.53
$[pyrHH]^+$	1.585	1.606	1.325	1.53
$[pyrH4]^+$	1.399	1.408	0.643	1.401
$[pyr14]^+$	1.302	1.270	-2.458	1.360

In Table S1, experimentally obtained densities are shown against those obtained from classical molecular dynamics (MD) simulation in the constant-NPT ensemble to validate the force field used. In the present study, charges on the ions were scaled to an absolute value of 0.8. NPT densities obtained from classical MD simulations, for the pure ILs and 0.1 M $[Li]^+$-doped solutions, with unit charges are also presented for comparison.

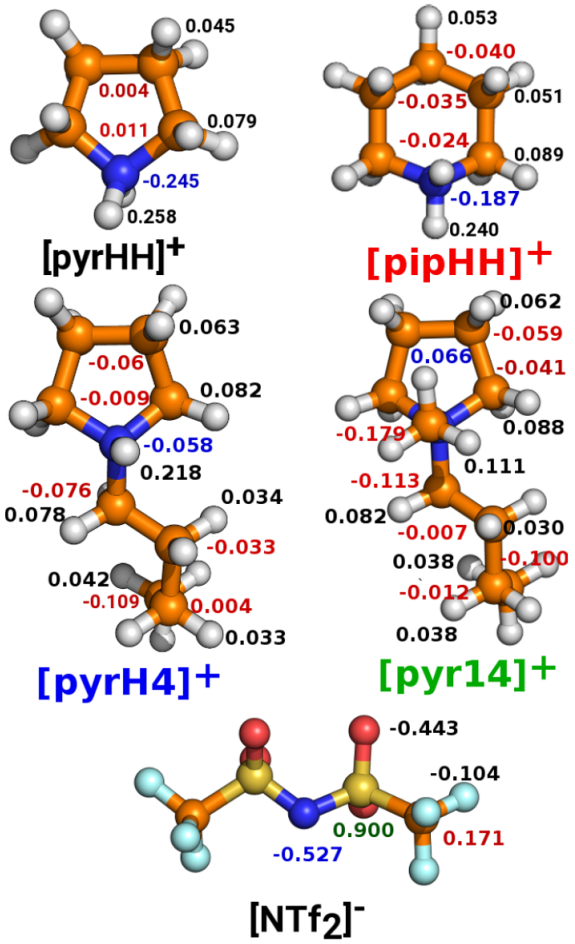

Figure S1: Ball-and-stick representations of the considered ions with the corresponding calculated RESP charges on each of the atoms. For the sake of clarity, charges on the C, N, and S atoms are shown in red, blue and green respectively. The charges on the other atoms are shown in black. The most acidic protons of the cation, labeled H_n in Fig. 1 of the main manuscript, can easily be identified based on the relatively higher partial charges assigned to them.

Ball-and-stick representations of the various considered ions along with the RESP atomic charges are shown in Fig. S2.

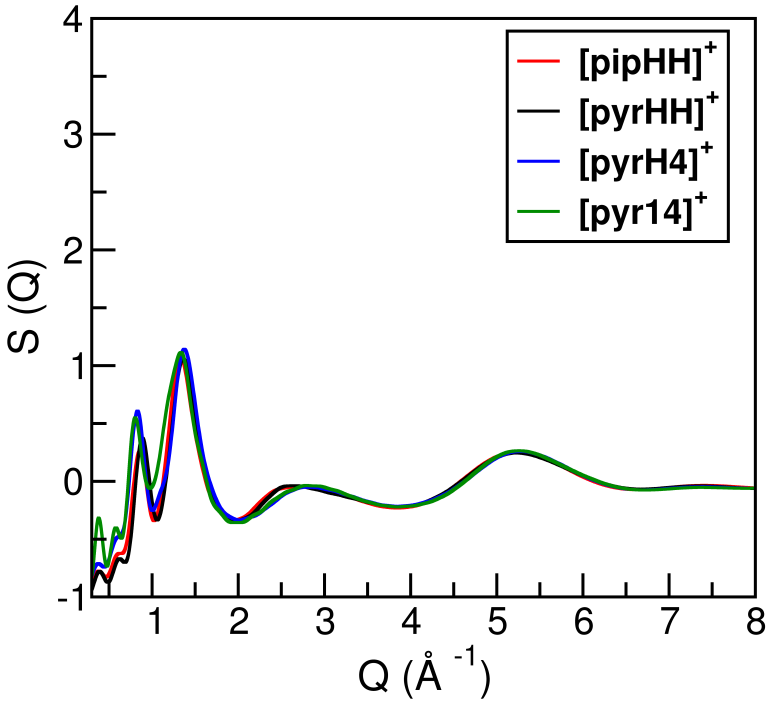

Figure S2: Total structure factors for x-ray diffraction of the four ionic liquids investigated. The structure factors predicted here qualitatively agree well with literature reproducing both the alkyl-chain dependent intermediate range order, in the low q region, as well as scattering contributions from the electron density on the anions observed in the high q region.[S1]

2 Ion-ion distributions

The three RDFs and the corresponding number integrals, shown in Fig. 2 of the main manuscript, are shown combined in the respective top and bottom panels of Fig. S3.

In the top panel of Fig. S3, ion-ion RDFs between the various ion types are shown; cation-anion using solid lines, anion-anion using dashed lines, and cation-cation using '+' symbols in order to depict the ordering pattern and illustrate the absence of a perfectly alternating structure since the maxima of the RDFs between like ions do not overlap perfectly with the minima of the RDFs between oppositely charged ions. In the bottom panel of Fig. S3, we demonstrate that the number integrals corresponding to cation-cation and anion-anion interactions actually intersect with those for the cation-anion interactions at distances approximately around the location of the end of the first cation-anion solvation shell: the

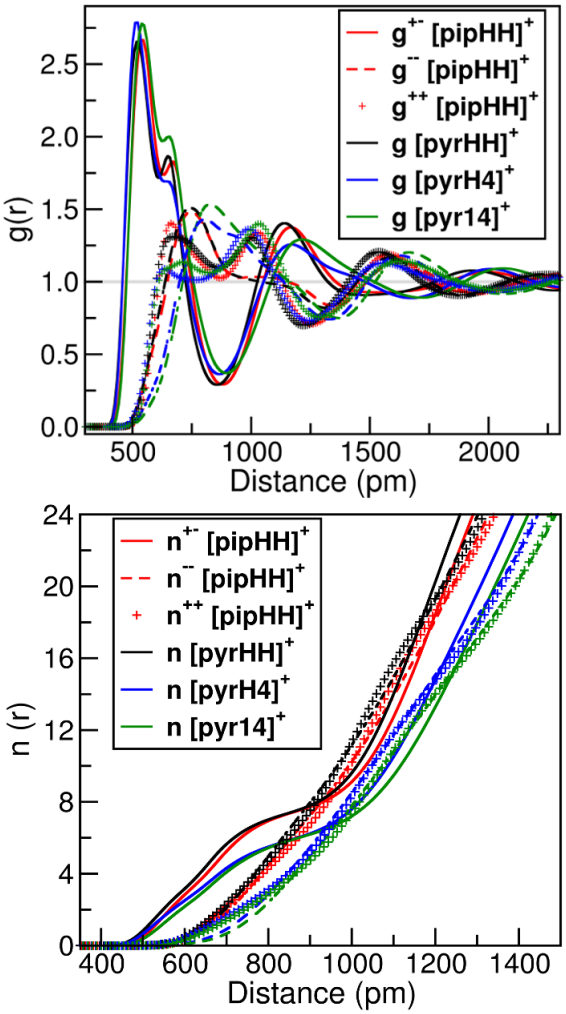

Figure S3: Cation-anion, anion-anion and cation-cation interactions in the investigated ILs. Top panel: corresponding RDFs between the representative coordinates of the ions (cation: ring center, anion: center of mass), bottom panel: corresponding number integrals.

distance at which the curves intersect is, of course, dependent on the strength of the inter-ionic interactions detailed in the manuscript.

In order to demonstrate the simultaneous solvation of both ion types by each other (a partial overlap of solvation shells as against a perfectly alternating arrangement of ions), CDFs showing three-body interactions with both ion types as reference are shown in Fig. S4.

Since the RDFs of distances from reference cations are comparatively inhomogeneous as against the anion-anion distributions, number integrals at specific cation-anion/ cation-cation distances (indicative of features in the graphs: shoulders, maxima and minima) are

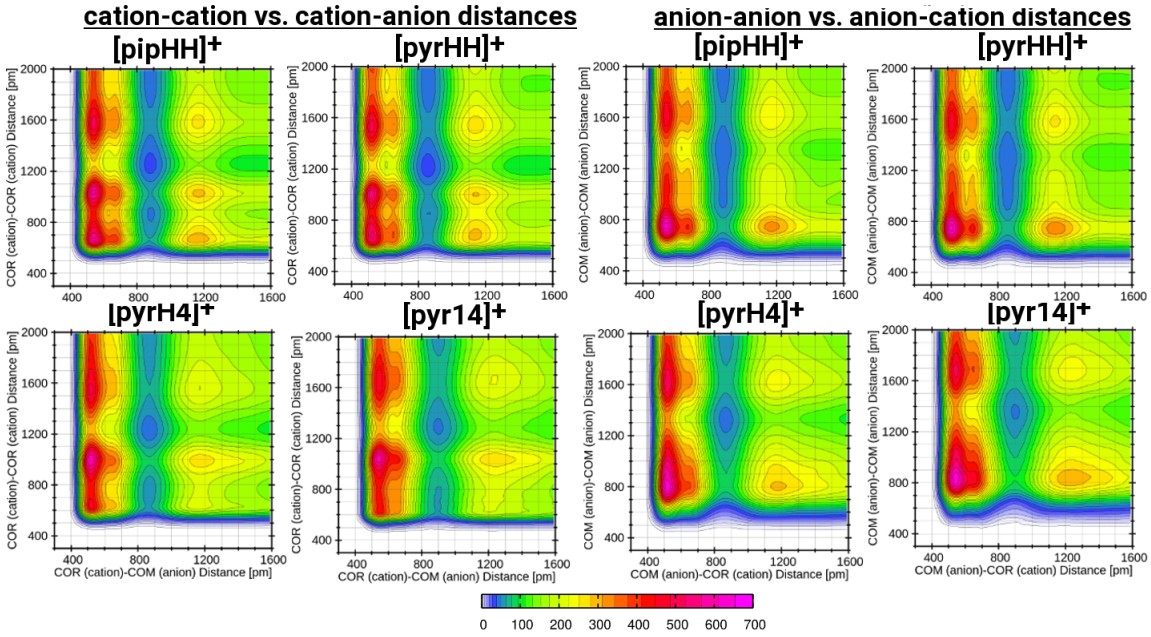

Figure S4: CDFs exhibiting three body interactions from a reference ion, distributions of distances between unlike ions on the x axis and between like ions on the y axis. Left panel: the cation is taken as the reference molecule, right panel: the anion is the reference molecule.

shown in Table S2.

Table S2: Cation-anion (n^{+-}) and cation-cation (n^{++}) coordination numbers and corresponding distances (shown within brackets) at the shoulders/ pre-peaks, maxima and end of the corresponding solvation shells respectively. Anion-anion coordination numbers are not shown herein as these distributions are more uniform and diffuse.

IL	n^{+-} (r)	n^{++}(r)
[pipHH][NTf_2]	1.42 (540), 4.41 (670), 7.21 (880)	1.55 (670), 11.49 (1030), 19.7 (1230)
[pyrHH][NTf_2]	1.26 (520), 4.32 (650), 7.33 (860)	1.67 (670), 11.07 (990), 19.9 (1210)
[pyrH4][NTf_2]	1.03 (520), 3.58 (660), 5.98 (870)	0.94 (640), 8.57 (1010), 15.5 (1220)
[pyr14][NTf_2]	1.02 (540), 3.08 (650), 5.91 (890)	1.54 (710), 8.38 (1030), 15.4 (1250)

3 H-bonding: N (cation)-O (anion) interactions

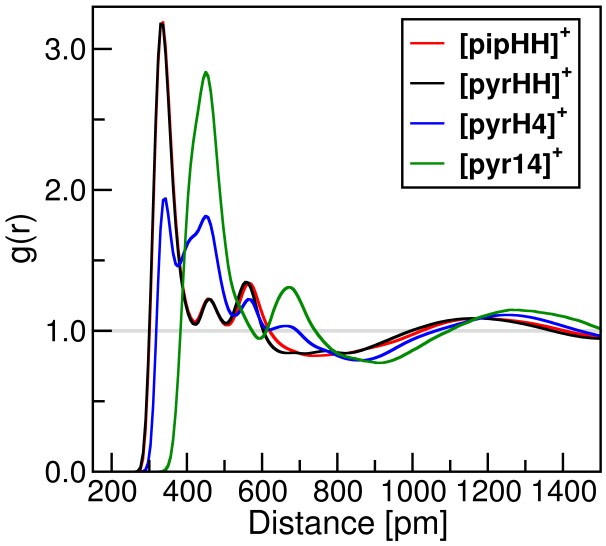

Figure S5: RDFs of distances between the N atoms of the heterocyclic cations and the O atoms of the anion (H-bond donor and acceptor).

To complement and complete the discussion on H-bonding in the protic ILs and to understand its implications on the aprotic IL, RDFs representing distances between the N atoms of the cations (the hydrogen atom donors) and the O atoms of the anions are shown in Fig. S5. Of course, the N atom on the cation in [pyr14][NTf_2] in not a H-bond donor but is shown for completeness. As mentioned in the manuscript, the graphs are shifted from the RDFs corresponding to H-bonds by abput 50-80 pm with the overall trends (outlined in the manuscript) remaining the same.

4 Anion flexibility

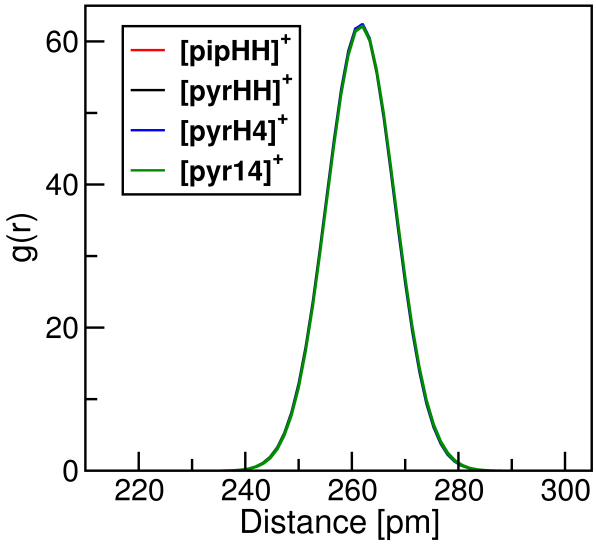

Figure S6: Intramolecular N-C RDFs within the anion showing the flexibility of the smaller anion and negligible influence of the cation therein.

In order to demonstrate the flexibility and the influence of the cation on the overall spatial characteristics of the anion, intramolecular RDFs between the central N atom and the terminal C atoms are depicted in Fig. S6.

5 Spatial distribution functions

Table S3: Maximal isovalues I_{max}, chosen isovalues I and resulting percentages P in % from the upper limit for SDFs isosurface intensities are shown for the investigated ILs [pipHH][NTf_2], [pyrHH][NTf_2], [pyrH4][NTf_2] and [pyr14][NTf_2].

	$[pipHH]^+$ ([pipHH][NTf_2])			$[pyrHH]^+$ ([pyrHH][NTf_2])			$[pyrH4]^+$ ([pyrH4][NTf_2])			$[pyr14]^+$ ([pyr14][NTf_2])		
Color	I_{max}	I	P	I_{max}	I	P	I_{max}	I	P	I_{max}	I	P
red	5.41	3.98	73.57	5.52	4.73	85.71	4.83	4.11	85.3	4.36	3.89	89.29
green	3.87	2.85	73.57	3.84	3.29	85.71	-	-	-	-	-	-
yellow	-	-	-	-	-	-	2.97	2.53	85.3	2.56	2.28	89.29
blue	-	-	-	-	-	-	2.97	2.53	85.3	2.56	2.28	89.29

The spatial distribution functions (SDFs) represent the three-dimensional density distribution of the previously defined subsets around a given reference molecule and are therefore used to study details of the spatial structure of the ILs cations within the liquids. The colors were chosen according to the polar and nonpolar entities in the systems: for all ILs, the anionic densities around the cations are shown in red. For [pipHH][NTf_2] and [pyrHH][NTf_2] the cationic densities are illustrated in green, while for [pyrH4][NTf_2] and [pyr14][NTf_2] the cationic desnities are divided into contributions from the polar head group of the cations in yellow and the nonpolar propyl group in blue. Here, the extent of the isosurface can be controlled by the so-called isovalue, which has to lie within a certain range. In general, a high isovalue leads to an isosurface considering only the density distribution of a subset very close to the observed molecule while a value approaching zero considers the density within the whole simulation box. The range is dependent on the number of molecules and atoms contributing to the density distribution. To nevertheless reach a comparable density representation, we considered the same percentage from the upper value limit of each range (cf. Table S3).

6 Voronoi analysis: surface coverage

Table S4: Surface coverage from Voronoi analysis for different ILs [pipHH][NTf_2], [pyrHH][NTf_2], [pyrH4][NTf_2] and [pyr14][NTf_2] by the constituent subsets A, CH and CT. The values are given as a percentage, so the sum of the coverages for each subset equal 100 %.

	A coverage			CH coverage			CT coverage		
IL	A	CH	CT	A	CH	CT	A	CH	CT
[pipHH][NTf_2]	39.5	60.5	-	83.7	16.3	-	-	-	-
[pyrHH][NTf_2]	43.0	57.0	-	88.1	11.9	-	-	-	-
[pyrH4][NTf_2]	27.0	46.7	26.2	66.4	10.0	23.7	51.0	32.4	16.7
[pyr14][NTf_2]	24.5	49.6	25.9	64.9	11.5	23.6	49.2	34.2	16.7

As a first approach to the results, it is meaningful to distinguish between the two ILs without side chain, i.e. [pipHH][NTf_2] and [pyrHH][NTf_2], and the two other ILs [pyrH4][NTf_2] and [pyr14][NTf_2]. For the former ILs, it can be seen that the coverage of A is dominated by the subset CH and the coverage of CH is dominated by A as one would expect from the typical structuring of particles with opposite charge. However, the coverage of A by its kind is much higher than the coverage of CH by its kind confirming the conclusions from the domain analysis that the anions structure is much more flexible than the structure of the cationic head group thus leading to higher self-interactions. The slight differences between [pipHH][NTf_2] and [pyrHH][NTf_2] probably originate from the difference in ring size and flexibility of the cationic head groups: for the bigger and more flexible piperidinium system, the coverage of both subsets A and CH is higher than for the smaller and more rigid pyridinium system. Since the identity of the anion and their amount is equal in both ILs, the corresponding values for A adjust to those for the CH subsets.

For [pyrH4][NTf_2] and [pyr14][NTf_2], the results are seemingly in good accordance with those for the previously discussed ILs; the coverage of A is dominated by the subset CH and vice versa. However, the presence of side chains in these two liquids leads to interesting structural details. For both ILs, the entities belonging to subsets A and CH are covered approximately

one fourth by units of subset CT, and the CT coverage is dominated for circa one half by the anions and one third by CH, which is of course also due to the covalent bond between CH and CT. This can be rationalized by considering the high flexibility of the side chains and the fact that the forming nonpolar domains, as seen from the domain analysis, are quite small and distributed and therefore completely surrounded by the polar network constituted by the subsets A and CH. Moreover, the nonpolar phases (represented by the subset CT) are not of spherical shape, which would minimize their surface area. Instead their surface is more broken up, thus allowing for more contacts to the polar subsets A and CH. However, the self-coverage for the entities from the CT subset is still remarkably high further emphasizing the microheterogeneous nature of these two ILs.

The smaller differences in the values between [pyrH4][NTf_2] and [pyr14][NTf_2] arise from the additional methyl group attached to the $[pyr14]^+$ cation leading to an increased CH coverage of the units from the subsets A and CT, while the remaining values for the remaining subsets A and CT adjust accordingly.

References

(S1) Li, S.; Banuelos, J. L.; Guo, J.; Anovitz, L.; Rother, G.; Shaw, R. W.; Hillesheim, P. C.; Dai, S.; Baker, G. A.; Cummings, P. T. Alkyl chain length and temperature effects on structural properties of pyrrolidinium-based ionic liquids: a combined atomistic simulation and small-angle X-ray scattering study. *J. Phys. Chem. Lett.* **2011**, *3*, 125–130.